ADVANCED BOARD LEVEL MODELING FOR WAFER LEVEL PACKAGES

Tiao Zhou, Ph.D.
Southern Methodist University
Dallas, TX, USA
tiaoz@smu.edu

Zhenxue Han, Ph.D.
University of Texas at Arlington
Arlington, TX, USA

Tingge Xu, and Hongbing Lu, Ph.D.
University of Texas at Dallas
Dallas, TX, USA

Kenna Wang
Creekview High School
Carrollton, TX, USA

ABSTRACT
In finite element analysis (FEA) of board level temperature cycling (TC) or drop test (DT) for wafer level packaging (WLP), the printed circuit board (PCB) is often simplified as a homogeneous material. The PCB effective elastic modulus is one of the key properties required for FEA. It is obtained from tensile test, bending test, or calculation. The tensile and flexural moduli however, often have significantly different values. The FEA results thus can be inaccurate if PCB modulus is not chosen properly. In this paper, the effects of PCB stackup, metal contents and metal trace orientations on effective tensile and flexural moduli are studied. It is determined that the effective flexural modulus depends on the stackup and it often does not correlate with the effective tensile modulus. Observations are made to assess if the PCB deformation is tension/compression dominant or bending dominant during TC and DT. Guidelines for effective elastic modulus calculation from tensile and flexural moduli are given in order to minimize the error in FEA of WLP board level TC and DT.

Key words: FEA, PCB, Solder joint reliability, WLP

INTRODUCTION
Predictive modeling has been widely used in packaging industry to reduce the development cycle time and optimize reliability [1]-[10]. In finite element analysis (FEA) of board level temperature cycling (TC) or drop test (DT), the printed circuit board (PCB) is often simplified as a homogeneous material to reduce the computation time. The effective elastic modulus is the key material property needed for FEA. It is be obtained through tensile or bending test [11]-[13]. The effective moduli can also be calculated manually, through FEA or Chen's laminate theory [14]. It is observed that the effective tensile modulus and flexural modulus values can be significantly different for a PCB. Is it reasonable to consider the PCB as a homogenous material in the mechanical modeling? Which modulus should be used as the effective modulus, tensile or flexural modulus?

In this paper, the effects of PCB details on effective modulus and error in FEA due to the choice of effective modulus are studied through tests and numerical analyses. It is demonstrated that the effective flexural modulus depends on the PCB stackup and it does not correlate with the effective tensile modulus. To study the effect of PCB modeling approach on finite element simulation results of WLP, a four layer PCB is modeled using the following three approaches:

A. a multilayer composite
B. a homogenous material using the tensile modulus as the effective elastic modulus
C. a homogenous material using the flexural modulus the effective elastic modulus.

The strain energy density (SED) and peeling stress of solder joints are compared for TC and DT FEA, respectively. Errors induced by the modeling approaches B and C are addressed. Observations are made to assess if the PCB deformation is tension/compression dominant or bending dominant, and if the choice of effective modulus is associated to such PCB deformation characteristics. At the end, the guidelines on effective elastic modulus calculation from tensile and bending moduli are given in order to minimize the error in the finite element simulations of board level TC or DT for WLP.

PCB MATERIAL CHARACTERIZATION

In this session, elastic moduli of selected PCB's are obtained through tests to illustrate the difference between the tensile modulus and flexural modulus. Trends of the elastic moduli are obtained through numerical analysis to further understand the effects of PCB construction and design.

Experiment

A JEDEC drop test board is used for this characterization. The stackup is depicted in Figure 1. The samples are prepared by routing the PCB along the major axis (type A) and minor axis (type B). The sample width is 12.7 mm (Figure 2). And the sample thickness is 1 mm.

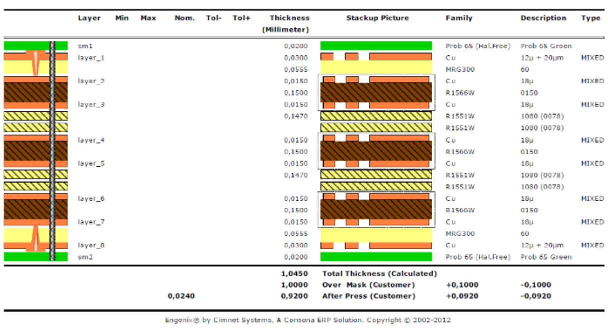

Figure 1. Stackup of the PCB.

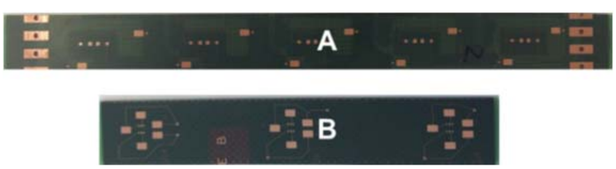

Figure 2. PCB Test Samples Type A 133x12.7 mm and Type B 77x12.7 mm.

Tensile test [11] is performed to determine the effective tensile modulus. 3 point bending test [12] is used to determine the effective flexural modulus. The elastic moduli obtained from both tests are listed in Table 1. The flexural moduli for groups A and B are approximately the same. Tensile modulus is measured only for group A samples.

It is seen that the measured flexural modulus is significantly lower than tensile modulus. The flexural modulus of a PCB which is a highly anisotropic laminate is a critical function of stackup, it does not necessarily correlate with the tensile modulus, which is not stackup dependent. In order to further demonstrate the stackup dependency and trends with respective to designs, the moduli of three stackup options are calculated with FEA and Chen's Laminate Theory [14]. This is discussed next.

Table 1. Average Tensile and Flexural Moduli Obtained from Tests.

	Group A Samples 	Group B Samples 
Tensile Modulus E	27.2 GPa	
Flexural Modulus E_B	15.8 GPa	15.4 GPa

Elastic Modulus Trends

To simplify the study, a four layer design is considered. This design is different from the one used for testing discussed above. The total thickness is 1.020 mm. Three stackup options are considered (Figure 3) to investigate the effect of PCB stackup. The thicknesses of the metal and soldermask layers are the same for all three stackups. The core thicknesses considered here are 240, 480 and 720 µm, respectively. The inner Cu layer placement is determined by the core thickness. The thicker the core, the closer the inner layers to the PCB surface. It is expected that the flexural modulus is higher with a thicker core since the inner Cu layers are farther away from the cross section natural axis.

Here the Cu content is assumed for the inner layers is assumed to be 70%.

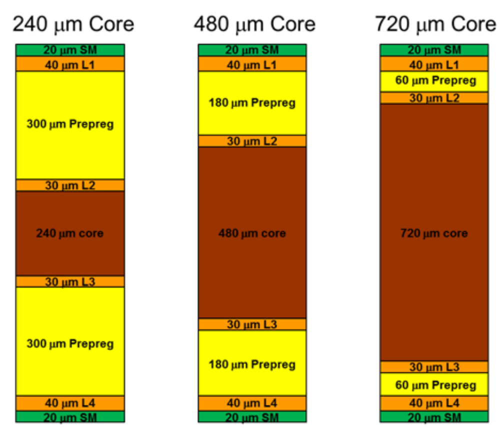

Figure 3. Three stackup options of a four layer design.

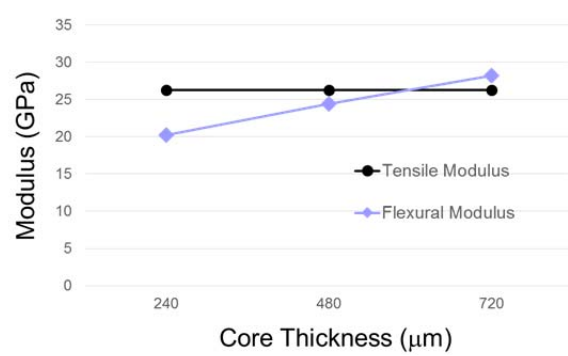

Figure 4. Tensile and Flexural Moduli for Three Stackup Options. 10% Cu content is assumed for L1 and L4.

The tensile and flexural moduli for the three stackups of one design are plotted in Figure 4. It is seen that the tensile modulus is identical to all three stackup options. However, the flexural modulus is not. It is higher with a thicker core.

At this point, it is of interest to further explain the stackup effect with FEA. Figure 5 shows the in-plan normal stress distributions of the three PCB's during tension and bending. It is seen that during tension the normal stress distribution (Figure 5a) of the Cu layers are the same for all three stackup options. This confirms that contribution of Cu layers to resistance the tension is the same for all stackups. Therefore, the tensile modulus does not change with stackup. The stress distribution in Cu during bending on the other hand, is stackup dependent (Figure 5b). With a thicker core, the inner layers are farther away from the neutral axis. The Cu layers are subjected to higher stress during the bending. They stiffen the board more compared to thinner core stackup, and this results in higher effective flexural modulus. The 720 µm core PCB has flexural modulus 28% higher than that of the 240 µm core PCB. The flexural modulus for 240 µm core stackup is lower than the tensile modulus, while the 720 µm core stackup is higher than the tensile modulus.

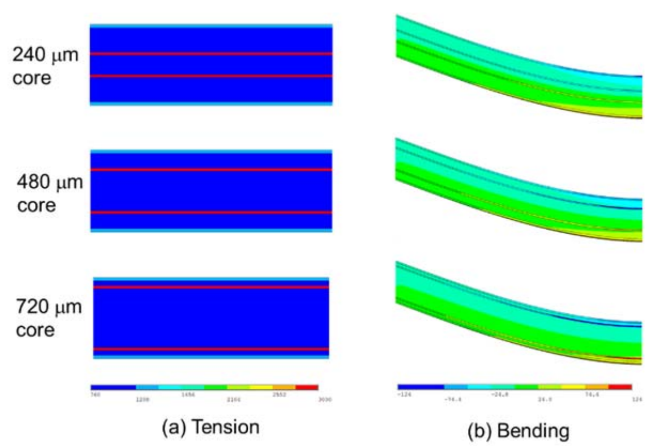

Figure 5. Stress Distribution of Boards with Three Different Stackups during Tension and Bending with Fixed Force. (a) Tension, and (b) Bending.

The elastic moduli as functions of outer layer Cu content are calculated and plotted in Figure 6. Both tensile and flexural moduli are linearly proportional to outer layer Cu content. The flexural modulus is more sensitive to outer layer Cu content than the tensile modulus. The change of flexural modulus due to outer layer Cu content variation is the same for all stackups.

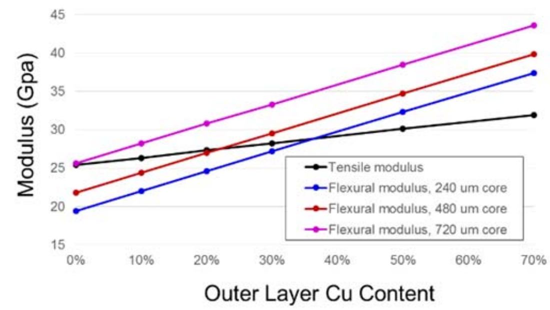

Figure 6. Effect of PCB Outer Layer Cu Content on Tensile and Flexural Moduli.

In the calculations above, the Cu distribution on the metal layers is assumed to be uniform. In applications however, individual traces are separated from each other and run in different orientations. To quantify this effect, tensile and flexural moduli as functions of Cu trace angle with respect major axis of the board sample are calculated and summarized in Figure 7. Here Cu content is assumed to be 30% for outer layers.

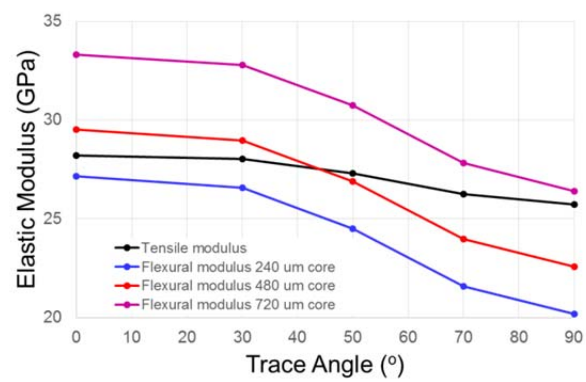

Figure 7. Effect of PCB Outer Layer Cu Trace Angle on Tensile and Flexural Moduli.

As are seen, both tensile and flexural moduli decrease with trance angle increase. The flexural modulus is more sensitive to the trace angle.

When calculating the PCB effective modulus by hand and with FEA, it is often assumed that the Cu distributions on the metal layers are uniform. This is equivalent to assumption of 0 trace angle which results in calculated effective moduli higher than their actual values.

Therefore, both test data and calculation have confirmed that the tensile and flexural moduli have different values. It is important to determine the appropriate effective elastic modulus to use in the FEA for accurate results. This will be discussed next.

EFFECT OF PCB MODULUS CHOICE ON TC AND DROP TEST FEA RESULTS

FEA is performed for both TC and DT to address two concerns:

1. Possible errors in FEA results by simplify the PCB as a homogeneous material, and
2. Recommended effective modulus to use when simplifying the PCB as a homogeneous material

Model Description

The WLP assembly consists a 12x12 ball array 0.5 mm pitch WLP and a four layer board. The PCB stackups considered are the same as the previous section. Due to symmetry, ¼ models are considered.

The key material properties are listed in Table 2. Here CTE of the core and prepreg are assumed to be the same as Cu. This is to simplify the analysis and de-couple the consideration of effective CTE calculation.

Table 2. Material Properties Used in TC and DT FEA.

	CTE (10^{-6}/°C)	Elastic modulus (Gpa)	Poisson's ratio	Density (kg/m^3)
Core	17	23	0.3	1950
Prepreg	17	23	0.3	1950
Cu	17	117	0.34	8890
Solder mask	60	3.2	0.32	1400
Silicon	2.7	130	0.28	2328
Solder	22	59.5	0.38	7200

For TC FEA, the PCB with size 2 mm larger than the package at every side is considered. Figure 8 shows the geometry and finite element mesh. -40/125°C temperature profile with 15 minute ramp and 15 minute dwell is considered. The solder material is SAC405 and is considered as a viscoplastic solid. The accumulated strain energy density (SED) per cycle of the 20 µm thick element layer next to WLP UBM is calculate and used as the damage indicator.

For DT FEA, a 77x77 mm four layer board is considered. The displacements are fixed at the mounting holes (Figure 9). The finite element mesh is shown in Figure 10. The solder joints here are modeled as cylinders to reduce the required computation resources. The input acceleration is a half sine pulse of 1500 Gs peak and 0.5 millisecond duration [15]. Dynamic response of the assembly is calculated for a duration of 5 milliseconds. The maximum peeling stress of solder at WLP side is calculated and used as the damage indicator.

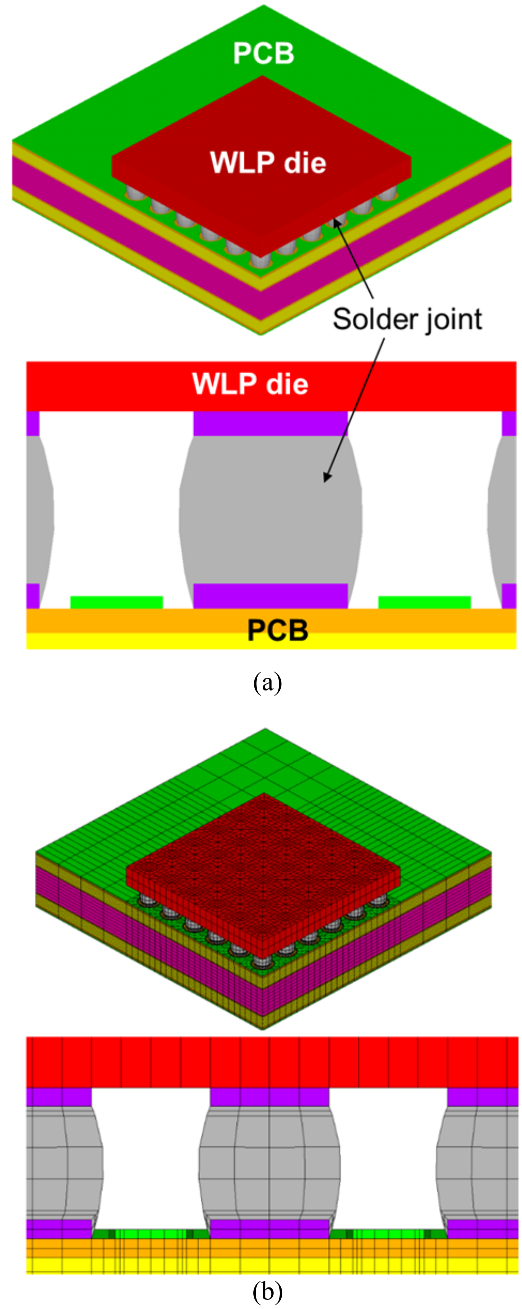

Figure 8. WLP Model (a) and Finite Element Mesh (b).

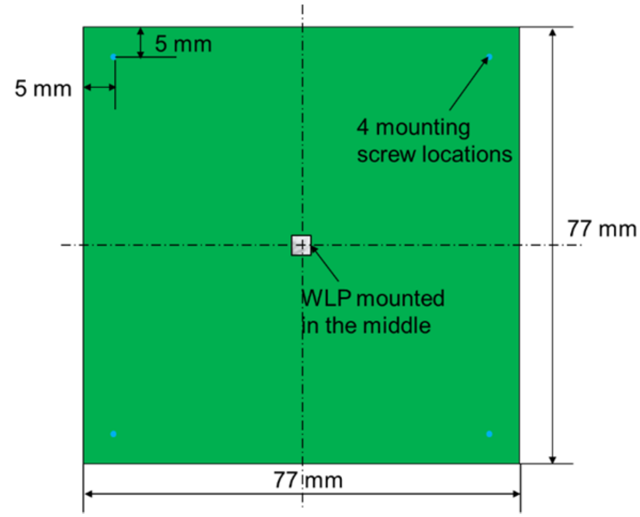

Figure 9. Illustration of DT Board Assembly.

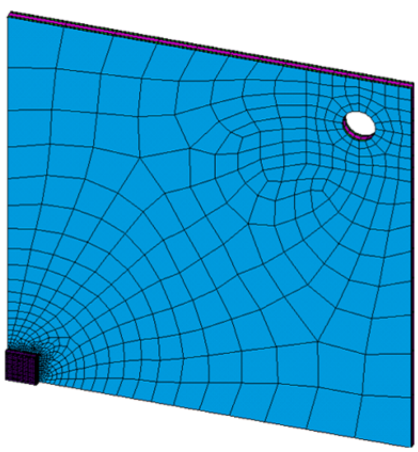

(a)

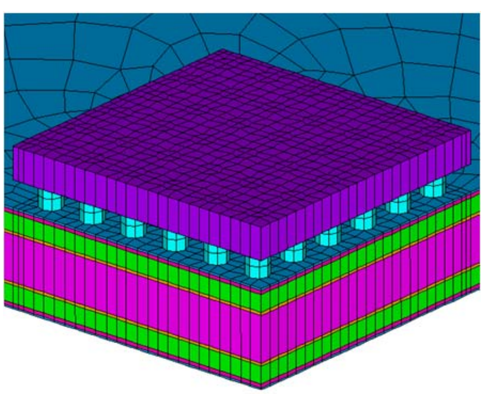

(b)

Figure 10. WLP Finite Element Model for DT. (a) Overall Mesh, and (b) Component Mesh.

TC FEA Results

A typical stress distribution is shown in Figure 11. It is seen that the maximum stress is at the corner joint. This joint is considered as the critical solder joint. Figure 12 shows the deformation (deformed shape) of the assembly at -40^{o}C. The PCB undergoes both bending and lateral shrinkage deformation. Both types of deformations contribute to solder joint stress. The right PCB effective modulus possibly has the components of both tensile and bending moduli. Therefore, it is interesting to understand the relationship between right effective modulus and the two moduli, tensile and flexural moduli. This is accomplished by investigating the effect of chosen PCB effective modulus on FEA results when modeling the PCB as a homogeneous material.

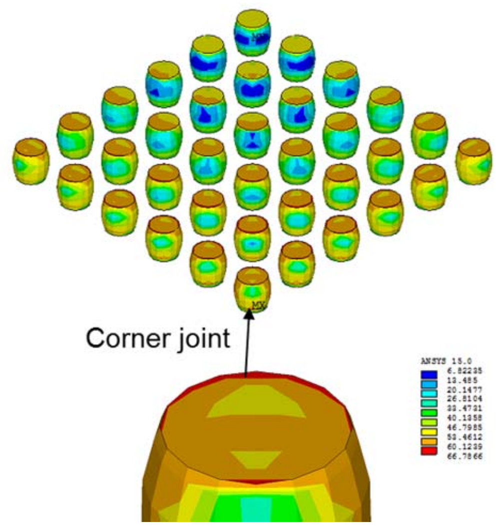

Figure 11. Typical Stress Distribution.

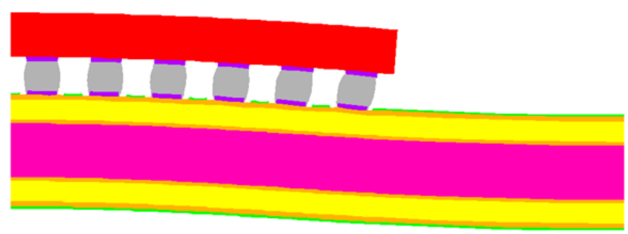

Figure 12. Assembly deformation at -40^{o}C.

The SED calculated using different PCB models for the three stackups are plotted in Figure 13. Here it is assumed that the SED calculated with detailed PCB model (A) produces the accurate results. SED deviations using homogeneous PCB models are compared against model A. It is seen from Figure 13 (a) that when approximating the PCB as a homogeneous material by using either tensile or flexural modulus results in error. Further effort is made to explore approaches to minimize the error by approximating the effective modulus with combinations of tensile and flexural moduli. These approaches include averaging these two moduli, and taking the greater of the two. The SED calculated hence are plotted in Figure 13 (b). It is seen that the average modulus still produces significant error as well. The greater modulus however, result in SED well approximate the detailed model.

Therefore, the greater of the tensile and flexural moduli is recommended to be used as the effective modulus when approximating the PCB as a homogeneous material for WLP TC FEA.

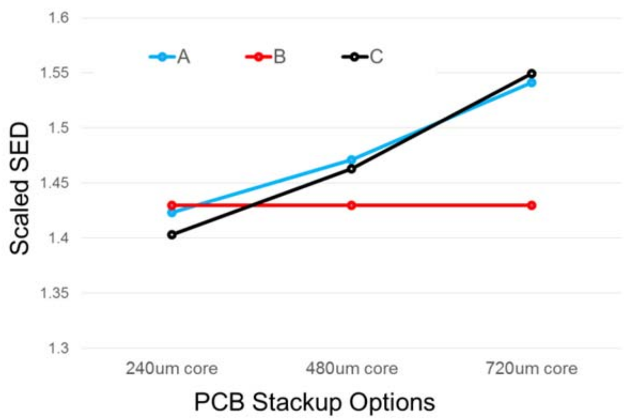

(a)

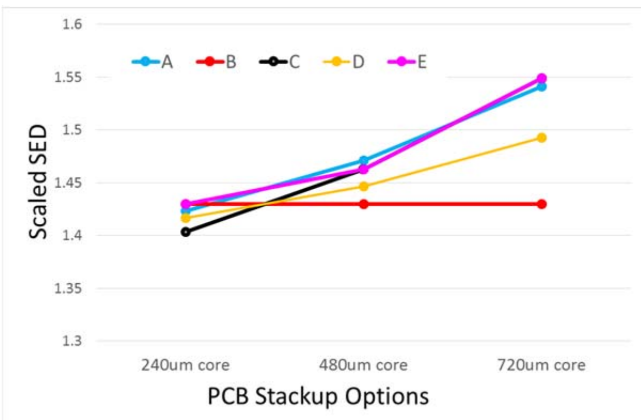

(b)

Model	PCB model	Effective Modulus Considered
A	Detailed	n/a
B	Homogeneous	Tensile modulus
C	Homogeneous	Flexural modulus
D	Homogeneous	Average of tensile and flexural moduli
E	Homogeneous	Higher one between the tensile and flexural moduli

Figure 13. SED Calculated with Detailed PCB model and Effective PCB Modulus. Inner Layers 70% Cu, Outer Layers 30% Cu.

DT FEA Results

A typical peeling stress distribution at solder joints for a DT model is shown in Figure 14. It is seen that the maximum stress is reached at the corner joint at the inner side (towards die center). This joint is considered as the critical solder joint. The maximum solder joint peeling stresses over 5 millisecond duration are calculated for different PCB models. The results are summarized in Figure 15. Here the results using detailed PCB model (A) are assumed to be accurate. It is seen that the homogeneous PCB models, with either the tensile modulus or the flexural modulus as the effective modulus produce some error. Among the six PCB options considered, the maximum error produced using homogenous PCB model with tensile modulus is 13%. It is 3% when using the flexural modulus as the effective modulus of the homogenous PCB model. Therefore, the flexural modulus should be used as the effective modulus when modeling the PCB as a homogeneous material in WLP DT FEA. This is related to the fact that PCB bending is the dominant deformation during DT.

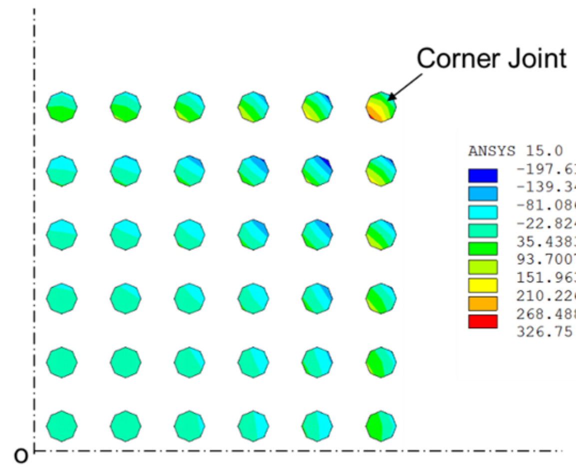

Figure 14. Typical DT Peeling Stress Distribution.

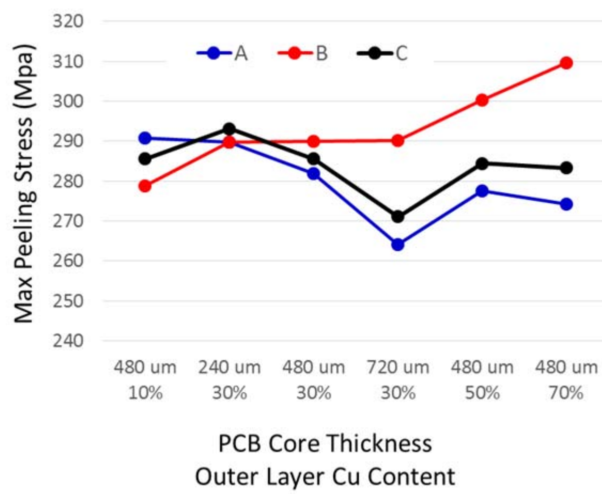

Model	PCB model	Effective Modulus Considered
A	Detailed	n/a
B	Homogeneous	Tensile modulus
C	Homogeneous	Flexural modulus

Figure 15. Maximum Peeling Stress at Solder Joints Calculated with Detailed PCB model and Homogeneous PCB Models.

By comparing Figures 6 and 15 it is apparent that the maximum peeling stress is inversely proportional to the effective elastic modulus. To further illustrate more data points for the design with 30% Cu on outer layers are calculated and plotted in Figure 16. This figure clearly confirm the trend.

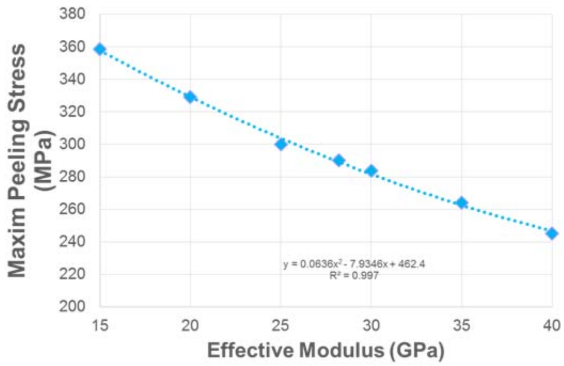

Figure 16. Maximum DT Peeling Stress as a Function of PCB Elastic Modulus.

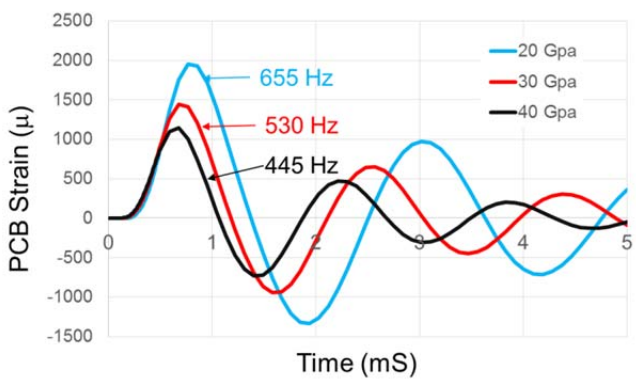

(a)

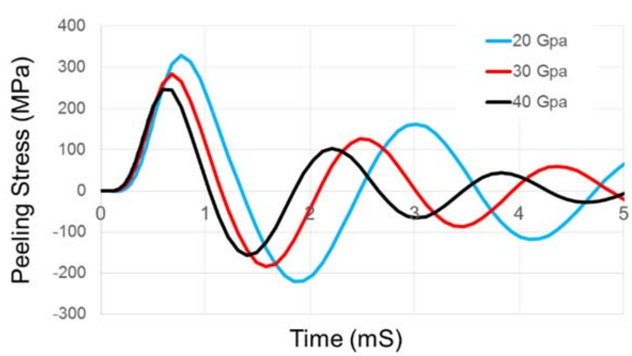

(b)

Figure 17. DT Response as Functions of Time for different PCB Stiffness Options. (a) PCB Strain near WLP Edge, and (b) Peeling Stress at Critical Solder Joints.

To understand the trend of peeling stress reduction with greater PCB stiffness, the PCB deformation and WLP solder joint stress are compared over time. Figure 17 shows the in-plane normal strain of PCB near WLP edge and the peeling stress histories at the critical solder joints. It is observed that the PCB resonant frequency increases while displacement magnitude decreases with greater elastic modulus (17a). The peeling stress (17b) varies overtime at the same frequency as the PCB. The peeling stress magnitude is proportional to PCB strain. This confirms that the peeling stress is induced by PCB bending during drop test. Evidently higher elastic modulus correlates to higher PCB resonant frequency and less PCB bending which in turn results in lower peeling stress.

CONCLUSIONS

PCB effective elastic modulus obtained from different methods are presented. The effect of choice of elastic modulus on FEA results is investigated. The following conclusions are made:

1. The values of tensile modulus and flexural modulus are different. The flexural modulus is stackup dependent while the tensile modulus is not.
2. Smaller trance angle on routing layers results in higher effective modulus. Using Cu content alone and ignoring trace routing detail overestimates the effective modulus.
3. When simplifying the PCB as a homogeneous material, using tensile or flexural modulus alone as the effective elastic modulus in both TC and DT FEA results in error. It is recommended that
    a. Use the greater of the tensile and flexural moduli as the effective modulus for TC
    b. Use the flexural modulus as the effective modulus for DT

ACKNOWLEDGEMENTS

Xu and Lu acknowledge the support of NSF under grant ECCS-1307997.

REFERENCES

[1] S. Chung, S. Oh, T. Lee, and M. Park, "Thermo-mechanical Analyses of Printed Board Assembly during Reflow Process for Warpage Prediction", Proc. of 15th International Conference on Thermal, Mechanical and Multi-Physics Simulation and Experiments in Microelectronics and Microsystems, 2014.

[2] R. Darveaux, "Thermal Cycle Fatigue Life Models for WLCSP Solder Joints", Proc. SMTAI, 2013.

[3] A, Syed, G. Sharon, and R. Darveaux, "Factors Affecting Pb-free Flip Chip Bump Reliability Modeling for Life Prediction", Proc. ECTC 2012.

[4] R. Darveaux and C. Reichman, "Solder Alloy Creep Constants for Use in Thermal Stress Analysis", Proc. SMTAI, 2012

[5] H. S. Dhiman, X. Fan and T. Zhou, "JEDEC Board Drop Test Simulation for Wafer Level Packages (WLPs)", Proc. ECTC, 2009.

[6] M. S. K. Rahim, T. Zhou and X. Fan, "Board Level Temperature Cycling Study of Large Array Wafer Level Package", Proc. ECTC, 2009.

[7] X. Fan, B. Varia and Q. Han, "Design and optimization of thermo-mechanical reliability in wafer level packaging", Microelectronics Reliability 50 (2010) 536–546.

[8] X. Fan, A. S. Ranouta, and H. S. Dhiman, "Effects of Package Level Structure and Material Properties on Solder Joint Reliability Under Impact Loading", IEEE Transactions on Component, Packaging, and Manufacturing Technology, Vol. 3, No. 1, Jan. 2013.

[9] T. Y. Tee, H. S. Ng, and Z. Zhong, "Design for Enhanced Solder Joint Reliability of Integrated Passives Device under Board Level Drop Test and Thermal Cycling Test", 5th EPTC Conference, Singapore, Dec. 2003, pp. 210-216.

[10] T. Y. Tee and H. S. Ng, "Design for Package and Board Level Reliability with CAE", SEMICON Singapore, Aug. 2003, pp. 59-67.

[11] ASTM standard D638 − 10, "Standard Test Method for Tensile Properties of Plastics".

[12] ASTM D 790-02, "Standard Test Methods for Flexural Properties of Unreinforced and Reinforced Plastics and Electrical Insulation Materials".

[13] ASTM D6272-10, "Standard Test Method for Flexural Properties of Unreinforced and Reinforced Plastics and Electrical Insulating Materials by Four-Point Bending".

[14] D. J. Chen and W. S. Chan, "Use of Composite Effective Moduli for Lumped Layers in Finite Element Analysis", Proc. of 13th AIAA SDM Conference, 2015.

[15] JEDEC Standard JESD22-B111, "Board Level Drop Test Method of Components for Handheld Electronic Products", 2003.